Investigating the physics of magnetic bright points by Sunrise/IMaX and Hinode/SOT data – work in progress

D. Utz, Instituto de Astrofisica de Andalucía - CSIC,Granada, Spain; IGAM, Institute of Physics, University of Graz, Austria, utz @iaa.es
J. Jurčák, Astronomical Institute of the Czech Academy of Sciences, Ondrejov, Czech Republic
S. Thonhofer, IGAM, Institute of Physics, University of Graz, Austria
B. Lemmerer, IGAM, Institute of Physics, University of Graz, Austria

Abstract
The well known solar activity is triggered and caused by extended solar magnetic fields. The most significant magnetic fields are present in the form of sunspots and sunspot groups and show the known 11 year activity pattern. Regardless of the importance of sunspots they are not the only observable magnetic features on the Sun. A whole spectrum of features exist going down to the smallest and yet very important small-scale features like magnetic bright points (MBPs). These features are known to science since the 1970s and huge progress in understanding and describing them was achieved. Nevertheless the complete physical picture from creation to disintegration is not well understood. We want to emphasize in the ongoing work on the disintegration part as it might yield new insights in the chromospheric and coronal heating problem. For that purpose, we study data sets from two instruments with high spatial resolution, balloon-borne mission - Sunrise – and a space-borne instrument – Hinode.

1. INTRODUCTION

Magnetic bright points (MBPs) are manifestations of small scale magnetic field concentrations seen in the photosphere in intergranular lanes (Berger and Title 2001). They were first found in the 1970s and since then observed and studied in more detail (Mehltretter 1974). They show sizes typically smaller than 200 km in diameter (Utz et al. 2009) and are highly dynamic with lifetimes in the range of minutes (Utz et al. 2010). While theoretical concepts explain their formation – convective collapse model (e.g. Spruit 1976); observed and verified in 2008 by Nagata et al. – there are no theoretical concepts and observations of how they dissolve and what happens to the stored magnetic field energy. To close this gap it is necessary to conduct studies of MBPs with the best available spectro-polarimetric data (temporal, spatial and spectral resolution). Furthermore the obtained results should be of statistical significance. Therefore results should be obtained on larger data sets and hence automated image analysis algorithms are needed. In this paper we want to outline our efforts so far to answer the discussed scientific question – What happens to the magnetic field energy of MBPs when they dissolve?

2. DATA

For our study we use data taken by two highly advanced and outstanding missions. One mission – Hinode – is a spacecraft designed for the investigation of the solar magnetic fields while the other mission – Sunrise - is a balloon-borne instrument that was flown in the stratosphere.

2.1 Hinode:

In this analysis we use data from Hinode (see Kosugi et al. 2007) Solar Optical Telescope (SOT, Tsuneta et al. 2008). The data were taken on the 20th of January 2007 and comprise BFI (broad-band filter imager) G-band images and SP (spectropolarimetric) data. The SP data consist of normal map scans obtained close to disc centre with a cadence of about 2

minutes and 10 seconds, a FOV of about 3.69 by 81.15 arcsec², and a spatial sampling of 0.16 arcsec/pixel with diffraction limited spatial resolution of 0.32 arcsec. The scans started at 6:55 UT on the 20th of January and finished around 7:57 UT giving a total of 29 scans.

The BFI instrument performed at the same time (starting at 6:54:31 UT and ending at 7:58:02 UT) observations in the G-band filter with the following characteristics: A FOV of 21.79 by 55.79 arcsec² with a binning of 1 to 1 leading to the maximum spatial sampling of 0.054 arcsec/pixel and a diffraction limited spatial resolution of 0.22 arcsec. The temporal cadence is 30 seconds.

2.2 Sunrise:

The Sunrise mission was a one meter telescope flown on a balloon in the stratosphere (about 30 km above sea-level) in June 2009 (for a detailed mission description see Barthol et al. 2011). The scientific payload consisted of two instruments:

SuFI, the Sunrise Filter Imager, an instrument designed to observe the solar atmosphere (photosphere and chromosphere) in the near-ultraviolet and visible in 5 wavelength bands (214 nm, 300 nm, 312 nm, 388 nm - Cn band head - and 397.6 nm – Ca II H). The FOV of the instrument is approximately 15 by 40 arcsec².

The other instrument onboard the gondola is IMaX – Imaging vector Magnetograph eXperiment which conducts observations of doppler shifts and polarization in the Zeeman-sensitive photospheric spectral line of neutral iron at 525.02 nm.

In our study we used IMaX data from the 9th of June 2009. The data were taken between 0:36 UT and 2:02 UT and comprise two data sets (the first one ending at 0:58 UT and the second one starting at 1:31 UT). Both data sets were recorded in the V5-6 mode. This mode comprises all 4 polarization states and 5 wavelength samples around the iron line center (-80 mÅ, -40 mÅ, 40 mÅ, 80 mÅ and 227 mÅ – continuum) accumulated within 6 single exposures (for more details about IMaX see Martinez Pillet et al. 2011).

3. ANALYSIS

Nowadays the advent of space-borne instruments gives us on the one side the ability to obtain highly resolved stable longtime observations but on the other hand leads to enourmous amounts of data. To be able to analyse such data sets it is highly recommendable to use automated computer algorithms. In the recent years we developed an automated MBP identification and tracking algorithm as described in Utz et al. 2009 and 2010. At the moment the programme developement concentrates on an interface for the SIR (Stokes inversion by response functions) code developed by Ruiz Cobo and del Toro Iniesta in 1992. These two codes will be used subsequently for the analysis of the Hinode and Sunrise data. In the following we will discuss the current state of the art of our project.

3.1 Hinode:

At the moment we are working on the implementation of a GUI (graphical user interface) for the SIR code. The principle development has successfully ended and first automated inversions of complete data sets are underway. The huge advantage of the developed add-on for the SIR code is the possibility to a) invert complete image scans instead of single pixels b) to have an easy access to the control parameters and c) to obtain the resulting inversion parameters in standardized FITS (flexible

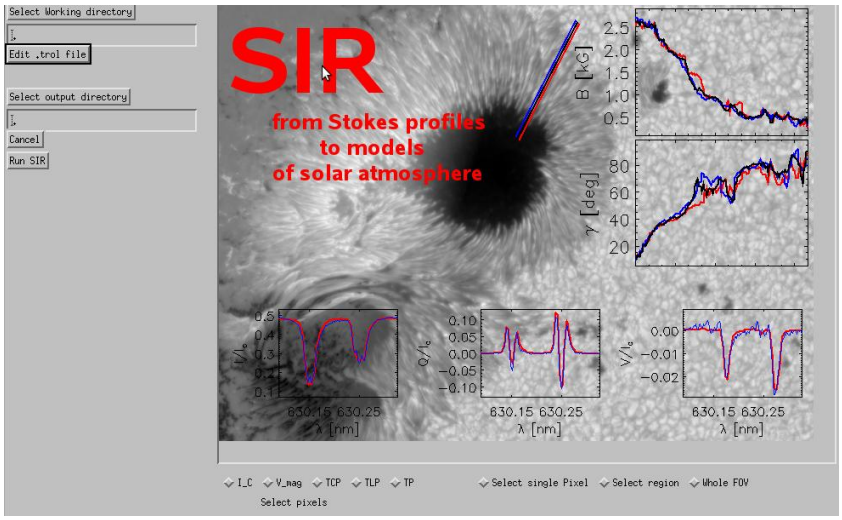

Fig. 1. The GUI add-on for the SIR code. On the left hand side the working directory, the output directory and the inversion control file can be selected and modified. On the lower edge of the starting screen, options for pre-inversion snapshots are shown. E.g. it is possible to give an overview of the intensity of the selected data or the total polarisation. Furthermore a subfield of the data set can be selected for inversions.

information transport system) files. Figure 1 shows the current status of the GUI while Fig. 2 gives a snapshot detail of an inverted temperature and velocity map of the Hinode/SP data set. For more details about the software add-on to the SIR code see Thonhofer et al. 2012.

Furthermore we worked on inversions of single MBPs (as the GUI and automation add on for the SIR code has not been ready at that moment). First inversion results of MBPs are promising and can be seen in Fig. 3. The figure demonstrates the evolution of a selected MBP in the G-band filtergram (first row; SOT/BFI) from left to right. The next rows show the different SP maps: Continuum intensity, temperature at optical depth log(τ) = -1.3 (between 4800 K and 5700 K), magnetic field strength (scaled from 30 G to 200 G), inclination angle (between 30 deg and 150 deg), and the line-of-sight velocity (between -2 km/s and 2 km/s). Except of the continuum intensity the parameters were obtained by using the SIR code. Clearly the MBP is associated with strong magnetic

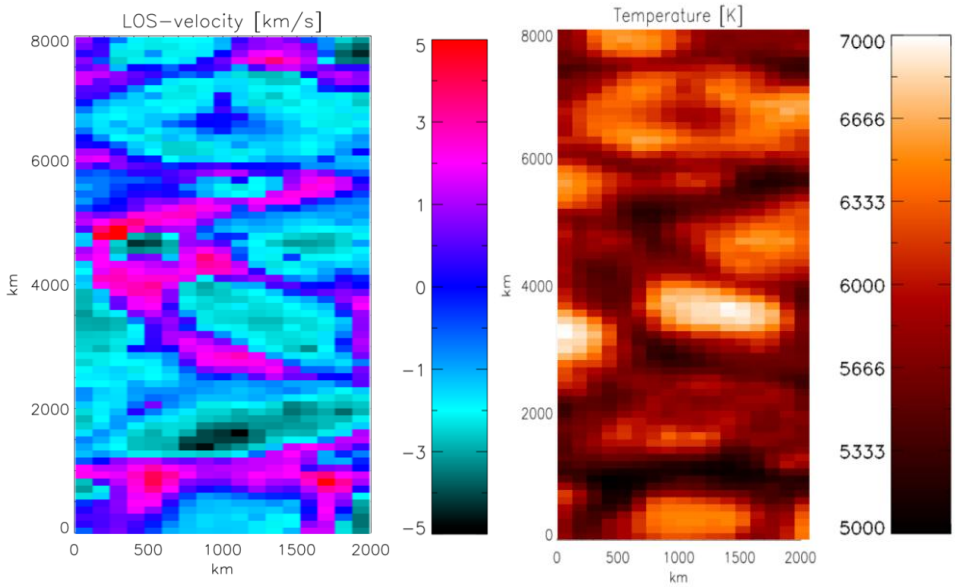

Fig. 2.: left: a small detail of the velocitiy map. The map was obtained by the SIR code and shows clearly the granulation pattern. Granules are given in blue (upstreaming plasma) while the intergranular plasma is given in red/pink colors (downflows). right: The same detail as on the left hand side but for the temperature map. The granules can be seen again as hot and bright features with temperatures up to 7000 K while the intergranular regions have only temperatures of about 5000 K.

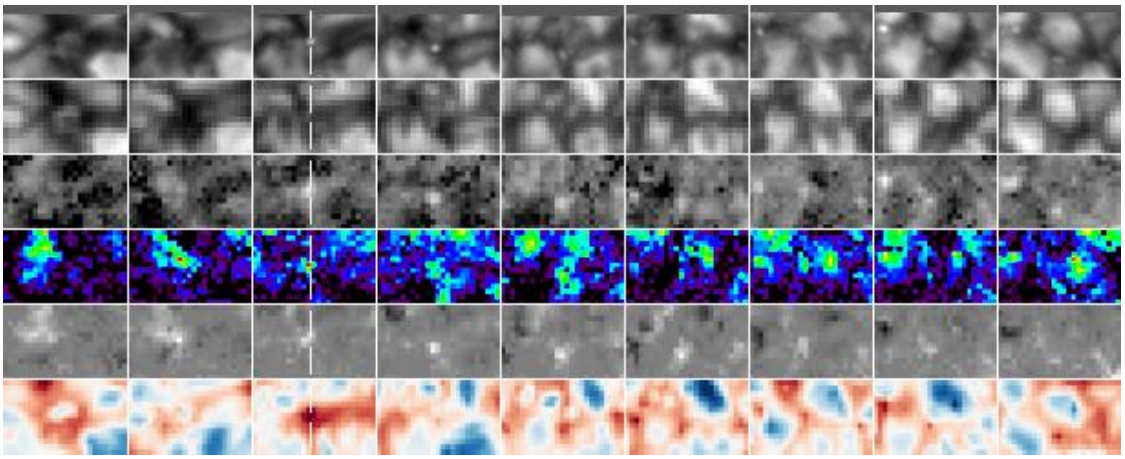

Fig. 3. The evolution of a selected MBP in the G-band and in selected physical parameter maps obtained from inversions. From top to bottom: The G-band intensity with an evolving MBP (marked in the 3rd image from left by a vertical line), the SP continuum intensity, the temperature map, the magnetic field strength, the magnetic field inclination and finally the line-of-sight velocity component.

fields and in the moment of its appearance with a strong downflow. This was already observed by Nagata et al. 2008.

3.2 Sunrise:

To verify obtained results and increase their statistical significance it is always important to cross-check results with independent data sets. An even better way is to cross-check results with independent instruments. Hence we started to analyse Sunrise/IMaX data sets. We applied the automated MBP identification algorithm (Utz et al. 2010) on the continuum images (see Fig. 4). From this figure it is clear that the algorithm identifies in the continuum two types of features: non-magnetic small granules and MBP features. The first row of the figure shows the continuum intensity of 2 examples. The second row illustrates the V/I polarisation within the iron line clearly indicating that the left hand feature is a non-magnetic small granule while the right hand feature is a small-scale magnetic field concentration – MBP.

We investigated the intensity normalised to the continuum intensity (continuum line profile; sampled with 4 measurement points + continuum). The line profiles are shown in the third row of the figure (panel 1 and 3). One can see that magnetic features look enhanced in intensity within the line profile compared to non magnetic features. This can be seen in the line profiles displayed in panel 1 and 3 of the third row and the relative strengths of the line depressions.

We used this relative intensity enhancement to distinguish between magnetic and non magnetic features and hence are able to solely identify MBP features in the data set. In the following we want to discuss two of the found cases:

Case I shows a brightening in the continuum without any corresponding magnetic field signal (V/I polarisation) in the beginning (see Fig. 5). Later on a strong magnetic field develops on the position of the brightening while the brightening itself decreases. This might be a case of MBP formation with strong downflows as discussed in the paper of Nagata et al. 2008.

Case II shows two opposite polarities very close to each other (see Fig. 6). One polarity (shown in bright color) is quite weak and disappears during the evolution of the brightness enhancement in the continuum. This might indicate a reconnection event on small scales. More information can only be obtained with inversions and inverted data which will be done in the near future.

4. CONCLUSION AND OUTLOOK

In this proceeding we have shown the current state of our investigations on MBPs. We are working on an automated image inversion add-on for the SIR inversion code. The next steps would be:

- Implementation of an automated faulty-pixel-detection and reinversion of the faulty pixels
- Exhaustive tests of the achieved inversion quality
- Parallelisation of the code to improve the runtime performance
- Automated detection of the type of the

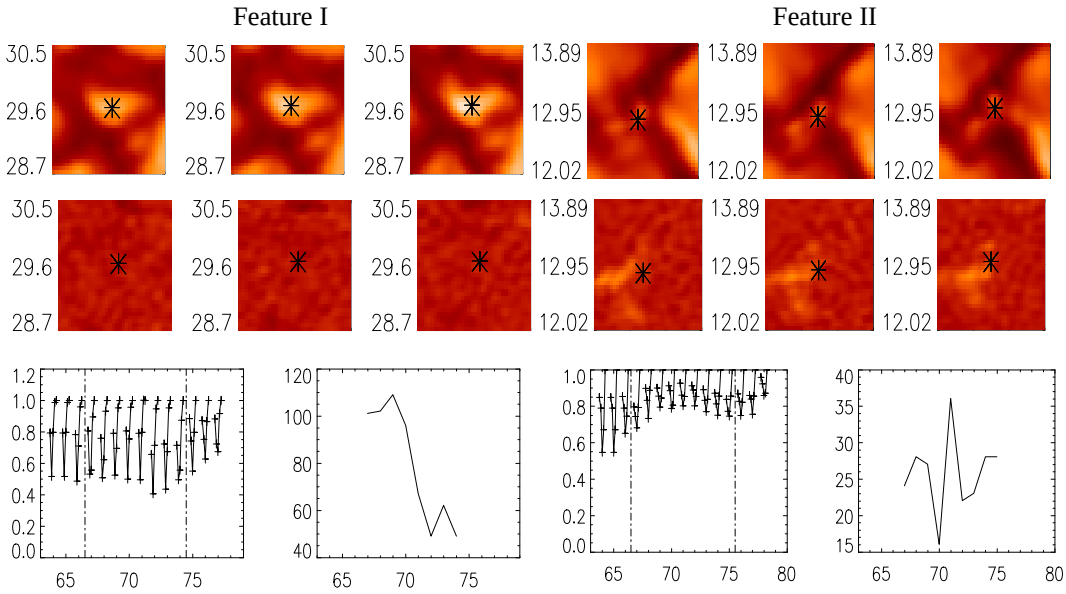

Fig. 4.: First row: shows the continuum intensity of the IMaX data set with two identified structures (first 3 images first feature; next 3 images second feature). Second row: shows the V-polarisation signal of the same FOV region. Clearly the first feature is a non magnetic small granule while the second feature is a correctly identified MBP. Third row: The normalised intensity to the continuum intensity is shown (first and third panel); Clearly non magnetic features appear darker in the samples within the iron line profile compared to magnetic features. Second and fourth panel show the evolution of the size of the identified structure.

inversion region (quiet sun, plage region, umbra, penumbra)

Regarding the analysis of MBPs we have shown first results on a single MBP. In the future we want to apply the automated inversion to get good statistical parameters on interesting parameters like the line of sight velocity component and its relationship to the magnetic field strength. Of special interest for our research would be of course the evolution of the temperature with the line-of-sight velocity and the magnetic field strength at the end of the lifetime of the MBP. This could give insights into what is going on with and happening to the stored magnetic field energy at the end of the lifetime of the MBP. Is it used to heat the local plasma?

Regarding the Sunrise data the next step, which is underway, is the inversion of the data sets and the retrieval of physical meaningful parameters of MBPs. In this work we presented the possibility of the application of an automated algorithm for the identification of MBPs on IMaX continuum data and two promising case studies. One shows most probably the convective collapse taking place while the other case might demonstrate a small scale magnetic field reconnection.

Acknowledgements

We are grateful to the Hinode and Sunrise team for the possibility to use their data. Hinode is a Japanese mission developed and launched by ISAS/JAXA, with NAOJ as domestic partner and NASA and STFC (UK) as international partners. It is operated by these agencies in co-operation with ESA and NSC

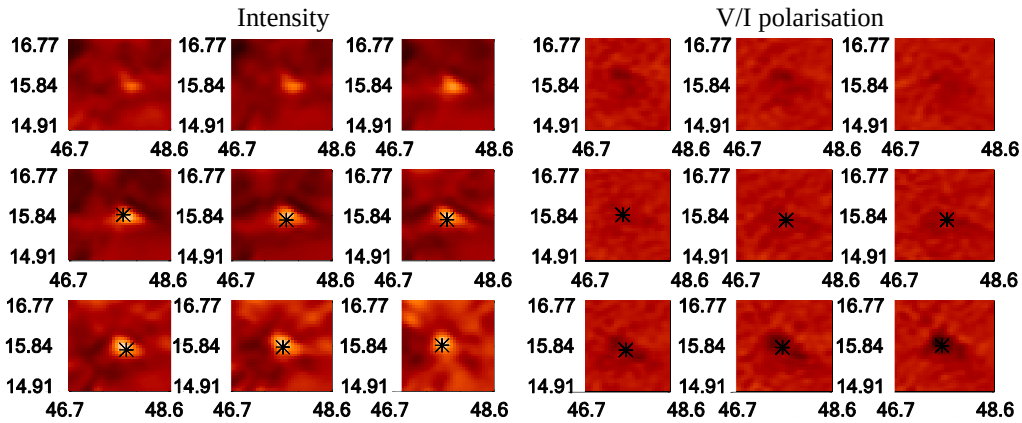

Fig. 5.: Left side (first three images of a row): the detail of the intensity map around an identified MBP feature. The feature itself is marked by an asterisk. Right side (the next three images): the temporal evolution of the same detail in the V/I polarisation map. The MBP feature is marked again by asterisks. In this specific example the brightening of the feature sets in before a clear indication of a strong magnetic field can be seen in the polarisation map. The shown image sequence has a cadence of 2 images/min.

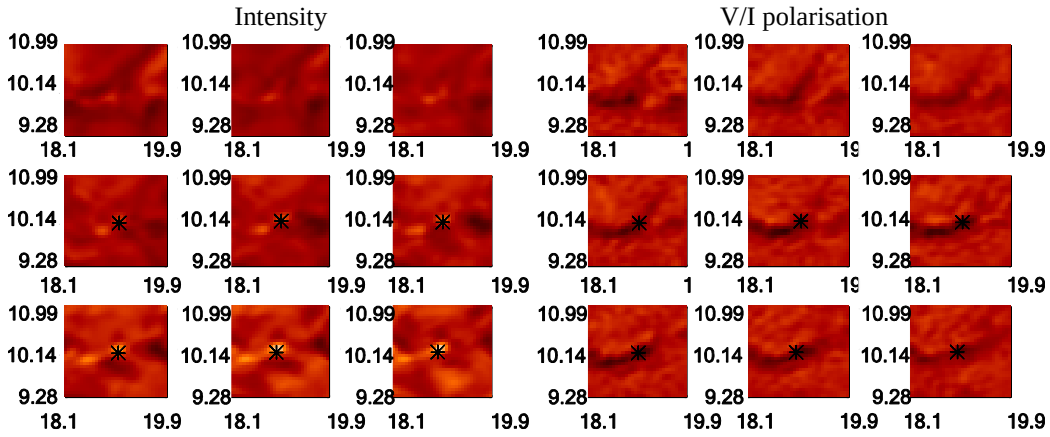

Fig. 6.: Similar to Fig. 5 but for the second case study. Here we show a possible reconnection event. In the first image of the V/I polarisation a negative and positive polarisation can be seen. The positive (bright) polarisation element spreads in the sucessive images out and seems to disappear. In the last row both polarisations get weaker while in the intensity images the brightness increases.

(Norway). The research was funded by the Austrian Science Fund (FWF): J3176 and P23618. D.U., S.T. and B.L. want to thank the ÖAD and MŠMT for financing a short research stay at the Astronomical Institute of the Czech Academy of Sciences in Ondrejov in the frame of the project MEB061109. Furthermore, J.J. wants to express vice versa his gratitude to the MŠMT and ÖAD for financing a short research stay at the IGAM belonging to the University of Graz.

REFERENCES

Barthol, P., Gandorfer, A., Solanki, S. K., Schüssler, M., Chares, B., Curdt, W., Deutsch, W., Feller, A., Germerott, D., Grauf, B., Heerlein, K., Hirzberger, J., Kolleck, M., Meller, R., Müller, R., Riethmüller, T. L., Tomasch, G., Knölker, M., Lites, B. W., Card, G., Elmore, D., Fox, J., Lecinski, A., Nelson, P., Summers, R., Watt, A., Martínez Pillet, V., Bonet, J. A., Schmidt, W., Berkefeld, T., Title, A. M., Domingo, V., Gasent Blesa, J. L., Del Toro Iniesta, J. C., López Jiménez, A., Álvarez-Herrero, A., Sabau-Graziati, L., Widani, C., Haberler, P., Härtel, K., Kampf, D., Levin, T., Pérez Grande, I., Sanz-Andrés, A., & Schmidt, E. 2011, The Sunrise Mission, *Solar Physics*, 268, 1-34. 10.1007/s11207-010-9662-9.

Berger, T. E. & Title, A. M. 2001, On the Relation of G-Band Bright Points to the Photospheric Magnetic Field, The Astrophysical Journal, 553, 449 – 469. Doi: 10.1086/320663

Kosugi, T., Matsuzaki, K., Sakao, T., Shimizu, T., Sone, Y., Tachikawa, S., Hashimoto, T., Minesugi, K., Ohnishi, A., Yamada, T., Tsuneta, S., Hara, H., Ichimoto, K., Suematsu, Y., Shimojo, M., Watanabe, T., Shimada, S., Davis, J.M., Hill, L.D., Owens, J.K., Title, A.M., Culhane, J.L., Harra, L.K., Doschek, G.A., Golub, L.: 2007, The Hinode (Solar-B) Mission: An Overview. *Solar Physics*, 118. doi:10.1007/s11207-007-9014-6.

Martínez Pillet, V., Del Toro Iniesta, J. C., Álvarez-Herrero, A., Domingo, V., Bonet, J. A., González Fernández, L., López Jiménez, A., Pastor, C., Gasent Blesa, J. L., Mellado, P., Piqueras, J., Aparicio, B., Balaguer, M., Ballesteros, E., Belenguer, T., Bellot Rubio, L. R., Berkefeld, T., Collados, M., Deutsch, W., Feller, A., Girela, F., Grauf, B., Heredero, R. L., Herranz, M., Jerónimo, J. M., Laguna, H., Meller, R., Menéndez, M., Morales, R., Orozco Suárez, D., Ramos, G., Reina, M., Ramos, J. L., Rodríguez, P., Sánchez, A., Uribe-Patarroyo, N., Barthol, P., Gandorfer, A., Knoelker, M., Schmidt, W., Solanki, S. K., & Vargas Domínguez, S. 2011, The Imaging Magnetograph eXperiment (IMaX) for the Sunrise Balloon-Borne Solar Observatory. *Solar Physics*, 268, 57-102. doi: 10.1007/s11207-010-9644-y

Mehltretter, J. P. 1974, Observations of photospheric faculae at the center of the solar disk, Solar Physics, 38, 43 – 57. Doi: 10.1007/BF00161822

Nagata, Shin'ichi, Tsuneta, Saku, Suematsu, Yoshinori, Ichimoto, Kiyoshi, Katsukawa, Yukio, Shimizu, Toshifumi, Yokoyama, Takaaki, Tarbell, Theodore D., Lites, Bruce W., Shine, Richard A., Berger, Thomas E., Title, Alan M., Bellot Rubio, Luis R., & Orozco Suárez, David 2008, Formation of Solar Magnetic Flux Tubes with Kilogauss Field Strength Induced by Convective Instability, The Astrophysical Journal, 677, 145 – 147. Doi: 10.1086/588026

Ruiz Cobo, B. & del Toro Iniesta, J. C. 1992, Inversion of Stokes profiles, The Astrophysical Journal, 398, 375 – 385. Doi: 10.1086/171862

Spruit, H. C. 1976, Pressure equilibrium and energy balance of small photospheric fluxtubes, Solar Physics, 50, 269 – 295. Doi: 0.1007/BF00155292

Thonhofer, S., Utz, D., Pauritsch, J., Hanslmeier, A., Jurčák, J., Lemmerer, B., Kühner, O.: 2012, Automated image inversion using SIR compared to MERLIN code. CEAB. in press

Tsuneta, S., Ichimoto, K., Katsukawa, Y., Nagata, S., Otsubo, M., Shimizu, T., Suematsu, Y., Nakagiri, M., Noguchi, M., Tarbell, T., Title, A., Shine, R., Rosenberg, W., Hoffmann, C., Jurcevich, B., Kushner, G., Levay, M., Lites, B., Elmore, D., Matsushita, T., Kawaguchi, N., Saito, H., Mikami, I., Hill, L.D., Owens, J.K.: 2008, The Solar Optical Telescope for the Hinode Mission: An Overview. Solar Phys. 249, 167 – 196. doi:10.1007/s11207-008-9174-z.

Utz, D., Hanslmeier, A., Möstl, C., Muller, R., Veronig, A., Muthsam, H.: 2009, The size distribution of magnetic bright points derived from Hinode/SOT observations. Astron. Astrophys. 498, 289 – 293. doi:10.1051/0004-6361/200810867.

Utz, D., Hanslmeier, A., Muller, R., Veronig, A., Rybák, J., Muthsam, H.: 2010, Dynamics of isolated magnetic bright points derived from Hinode/SOT G-band observations. Astron. Astrophys. 511, A39+. doi:10.1051/0004-6361/200913085.